

## Tunable hydrophobic eutectic solvents based on terpenes and monocarboxylic acids

Mónia Andreia Rodrigues Martins, Emanuel Almeida Crespo, Paula V.A. Pontes, Liliana P. Silva, Mark Bülow, Guilherme J. Maximo, Eduardo Augusto Caldas Batista, Christoph Held, Simao P. Pinho, and Joao A.P. Coutinho

*ACS Sustainable Chem. Eng.*, **Just Accepted Manuscript** • DOI: 10.1021/acsuschemeng.8b01203 • Publication Date (Web): 29 May 2018

Downloaded from <http://pubs.acs.org> on May 29, 2018

### Just Accepted

“Just Accepted” manuscripts have been peer-reviewed and accepted for publication. They are posted online prior to technical editing, formatting for publication and author proofing. The American Chemical Society provides “Just Accepted” as a service to the research community to expedite the dissemination of scientific material as soon as possible after acceptance. “Just Accepted” manuscripts appear in full in PDF format accompanied by an HTML abstract. “Just Accepted” manuscripts have been fully peer reviewed, but should not be considered the official version of record. They are citable by the Digital Object Identifier (DOI®). “Just Accepted” is an optional service offered to authors. Therefore, the “Just Accepted” Web site may not include all articles that will be published in the journal. After a manuscript is technically edited and formatted, it will be removed from the “Just Accepted” Web site and published as an ASAP article. Note that technical editing may introduce minor changes to the manuscript text and/or graphics which could affect content, and all legal disclaimers and ethical guidelines that apply to the journal pertain. ACS cannot be held responsible for errors or consequences arising from the use of information contained in these “Just Accepted” manuscripts.



# Tunable hydrophobic eutectic solvents based on terpenes and monocarboxylic acids

Mónia A. R. Martins<sup>1-4</sup>, Emanuel A. Crespo<sup>1,5</sup>, Paula V. A. Pontes<sup>4</sup>, Liliana P. Silva<sup>1</sup>, Mark Bülow<sup>5</sup>,  
Guilherme J. Maximo<sup>4</sup>, Eduardo A. C. Batista<sup>4</sup>, Christoph Held<sup>5</sup>, Simão P. Pinho<sup>2,3</sup>, and João A. P.  
Coutinho<sup>1,\*</sup>

<sup>1</sup>CICECO – Aveiro Institute of Materials, Department of Chemistry, University of Aveiro, 3810-193 Aveiro, Portugal

<sup>2</sup>Associate Laboratory LSRE-LCM, Department of Chemical and Biological Technology, Polytechnic Institute of Bragança, 5300-253 Bragança, Portugal

<sup>3</sup>Mountain Research Center – CIMO, Polytechnic Institute of Bragança, 5301-855 Bragança, Portugal

<sup>4</sup>Faculty of Food Engineering, University of Campinas, 13083-862 Campinas, Brazil

<sup>5</sup>Laboratory of Thermodynamics, Department of Biochemical and Chemical Engineering, TU Dortmund, 44227 Dortmund, Germany

\*Corresponding author: João A. P. Coutinho, E-mail address: [jcoutinho@ua.pt](mailto:jcoutinho@ua.pt), Phone: +351 234401507, Fax: + 351 234370084

## ABSTRACT

Recently some works reported claims that hydrophobic deep eutectic solvents could be prepared based on menthol and monocarboxylic acids. Despite of some promising potential applications these systems were poorly understood and this work addresses this issue. Here the characterization of eutectic solvents composed by the terpenes thymol or  $\iota$ (-)-menthol and monocarboxylic acids is studied aiming the design of these solvents. Their solid-liquid phase

1 diagrams were measured by differential scanning calorimetry in the whole composition range,  
2 showing that a broader composition range, and not only fixed stoichiometric proportions can  
3 be used as solvents at low temperatures. Additionally, solvent densities and viscosities close to  
4 the eutectic compositions were measured, showing low viscosity and that are less dense than  
5 water. The solvatochromic parameters at the eutectic composition were also investigated  
6 aiming at better understanding their polarity. The high acidity is mainly provided by the  
7 presence of thymol in the mixture, while  $\iota(-)$ -menthol plays the major role on the hydrogen-  
8 bond basicity. The measured mutual solubilities with water attest the hydrophobic character of  
9 the mixtures investigated. The experimental solid-liquid phase diagrams were described using  
10 the PC-SAFT EoS that is shown to accurately describe the experimental data and quantify the  
11 small deviations from ideality.  
12  
13  
14  
15  
16  
17  
18  
19  
20

21 **Keywords:** Terpenes, monocarboxylic acids, SLE, PC-SAFT, solvatochromic parameters,  
22 densities, viscosities, eutectic solvents.  
23  
24  
25  
26  
27  
28  
29  
30  
31  
32  
33  
34  
35  
36  
37  
38  
39  
40  
41  
42  
43  
44  
45  
46  
47  
48  
49  
50  
51  
52  
53  
54  
55  
56  
57  
58  
59  
60

## Introduction

Nowadays, developments in engineering and technology are strongly influenced by the concepts of *green chemistry* and *sustainability*. Within this framework, there is a demand for new eco-friendly solvents able to dissolve a large spectrum of solutes. Currently, one of the most important focus of research for novel solvents are the eutectic mixtures, and particularly the so-called deep eutectic solvents (DES).<sup>1</sup>

Most of the deep eutectic solvents proposed so far were prepared through the combination of materials from renewable resources with nontoxic and biodegradable compounds such as carboxylic acids,<sup>2</sup> polyols, and sugars;<sup>3</sup> being the vast majority hydrophilic. To the best of our knowledge, only a limited number of works reported hydrophobic eutectic mixtures.<sup>4-7</sup> However, in these studies, the solid-liquid phase diagrams were not characterized despite the relevant information that they can provide on the range of composition and temperature for operating these systems, while the physic-chemical characterization of their properties is also poor.

Due to their very low solubility in water and relatively low price,<sup>8</sup> terpenes appeared as good candidates to prepare sustainable and cheap hydrophobic solvents. Menthol and thymol are monoterpenoids used in various industrial processes and commercial products, and the use of their eutectic mixtures has been investigated. In the pharmaceutical field, mixtures of borneol/menthol,<sup>9</sup> and camphor/menthol<sup>10</sup> have been proposed as vehicles for transdermal delivery.<sup>11</sup> Moreover, mixtures of thymol with ibuprofen<sup>12</sup> or meloxicam;<sup>11</sup> and of menthol with ibuprofen,<sup>13</sup> testosterone,<sup>14</sup> lidocaine,<sup>15</sup> or ubiquinone<sup>16</sup> have been investigated as an analgesic, antimicrobial and anti-inflammatory vehicles.<sup>17</sup> Recently, mixtures of menthol and ibuprofen, benzoic acid, acetylsalicylic acid or phenylacetic acid were proposed as therapeutic deep eutectic solvents used to design a controlled drug delivery system using supercritical fluid technology<sup>18</sup> and as dissolution enhancers of active pharmaceutical ingredients.<sup>19</sup>

Combining terpenes and carboxylic acids, the menthol-lauric acid mixture was proposed as a hydrophobic DES able to extract indium from aqueous solutions;<sup>7</sup> and hydrophobic mixtures of menthol and naturally occurring acids, namely pyruvic acid,

acetic acid, L-lactic acid and lauric acid, were applied as solvents in the extraction of caffeine, tryptophan, isophthalic acid, and vanillin.<sup>17</sup> Furthermore, mixtures of DL-menthol with caprylic, capric and lauric acids were shown to be able to extract up to 80% of neonicotinoids from diluted aqueous solutions.<sup>5</sup>

The main goal of this work is to prepare and characterize eutectic mixtures composed by terpenes and monocarboxylic acids. The terpenes under study are L(-)-menthol and thymol, while as carboxylic acids caprylic, capric, lauric, myristic, palmitic and stearic acids are used. Solid-liquid phase diagrams of these mixtures are measured in the whole composition range, through differential scanning calorimetry (DSC) and described by the Perturbed Chain-Statistical Associating Fluid Theory (PC-SAFT) equation of state,<sup>20</sup> a molecular based approach able to explicitly take into account the association between the different constituents of the eutectic mixtures. Moreover, the densities, viscosities, solvatochromic parameters and mutual solubilities with water are measured at compositions close to the eutectic point. The experimental liquid densities are also predicted using PC-SAFT.

## Experimental

### Chemicals

Information on the studied compounds is summarized in Table 1 and Figure S1. The samples were used as received without further purification. The purity of the terpenes was evaluated by <sup>1</sup>H and <sup>13</sup>C NMR spectra and GC-MS.

**Table 1.** Compounds description and their melting properties herewith values from literature.

| Compound      | Supplier | CAS       | Purity wt% <sup>a</sup> | T <sub>m</sub> / K         |  | Δ <sub>m</sub> H / kJ·mol <sup>-1</sup> |                       |
|---------------|----------|-----------|-------------------------|----------------------------|--|---|-----------------------|
|               |          |           |                         | exp.                       | lit.                                       | exp.                                    | lit.                  |
| L(-)-menthol  | Acros    | 2216-51-5 | 99.7                    | 315.68 <sup>b</sup> ± 0.22 | 315.9 <sup>21</sup><br>316.7 <sup>21</sup> | 12.89 <sup>b</sup> ± 0.77               | 12.83 <sup>21</sup>   |
| Thymol        | Sigma    | 89-83-8   | ≥99.5                   | 323.50 <sup>b</sup> ± 0.34 | 323.1 <sup>21</sup><br>322.8 <sup>21</sup> | 19.65 <sup>b</sup> ± 0.42               | 17.54 <sup>21</sup>   |
| Caprylic acid | Sigma    | 124-07-2  | ≥99                     | 288.20 <sup>b</sup> ± 0.09 | 289.50 <sup>22</sup>                       | 19.80 <sup>b</sup> ± 0.54               | 21.38 <sup>22</sup>   |
| Capric acid   | Sigma    | 334-48-5  | 99-100                  | -                          | 304.75 <sup>23,b</sup>                     | -                                       | 27.50 <sup>23,b</sup> |
| Lauric acid   | Sigma    | 143-07-7  | ≥99                     | -                          | 317.48 <sup>23,b</sup>                     | -                                       | 34.69 <sup>24,b</sup> |
| Myristic acid | Sigma    | 544-63-8  | ≈95                     | -                          | 327.03 <sup>23,b</sup>                     | -                                       | 45.75 <sup>25,b</sup> |

|               |         |         |     |   |                        |   |                       |
|---------------|---------|---------|-----|---|------------------------|---|-----------------------|
| Palmitic acid | Aldrich | 57-10-3 | ≥98 | - | 336.84 <sup>23,b</sup> | - | 51.02 <sup>23,b</sup> |
| Stearic acid  | Merck   | 57-11-4 | ≥97 | - | 343.67 <sup>23,b</sup> | - | 61.36 <sup>23,b</sup> |

<sup>a</sup>Declared by the supplier; <sup>b</sup>Melting properties considered in the PC-SAFT modelling.

## Methods

### Mixtures Preparation

Binary mixtures of terpene and carboxylic acid were prepared by adding the compounds into glass vessels at different molar ratios in the full composition range, using an analytic balance XP205 (Mettler Toledo, precision = 0.2 mg). The mixtures were melted under stirring on a heating plate until a homogeneous liquid mixture was obtained and then cooled to room temperature. Samples (2 – 5 mg) were hermetically sealed in aluminum pans and weighed in a micro-analytical balance AD6 (PerkinElmer, USA, precision = 0.002 mg). Mixtures were analyzed by NMR spectroscopy at room temperature 48 h after their formation – Figure S2. No differences in the spectra or new NMR signals were observed 48 h after the formation of the systems, showing that esterification did not take place, thus proving the stability of the studied mixtures.

### Differential scanning calorimetry

The melting points of pure components and their mixtures were determined using a DSC 2920 calorimeter from TA Instruments working at atmospheric pressure and coupled to a cooling system. The equipment was previously calibrated with indium. The analytical procedure was based on a cooling ramp down to 208.15 K at 5 K·min<sup>-1</sup>, followed by a heating ramp up to 10 K above melting at 1 K·min<sup>-1</sup>. A constant nitrogen flow (purity ≥ 0.99999 mass fraction) was used as the purge gas to avoid condensation of water at low temperatures. Data were analyzed through the TA Universal Analysis software (TA Instruments) and the melting temperature taken as the peak temperature. At least three cycles of cooling and heating were performed for pure compounds and one cycle for mixtures.

### Density and viscosity

Densities and viscosities were measured at atmospheric pressure and in the temperature range (278.15 to 373.15) K using an automated SVM 3000 Anton Paar rotational Stabinger viscometer–densimeter (temperature uncertainty:  $\pm 0.02$  K; absolute density uncertainty:  $\pm 5 \times 10^{-4}$  g·cm<sup>-3</sup>; dynamic viscosity relative uncertainty:  $\pm 0.35\%$ ).

#### *Kamlet Taft Solvatochromic Parameters*

The solvatochromic parameters  $\pi^*$ ,  $\beta$  and  $\alpha$  were measured at 323.15 K by adding very small quantities of the probes *N,N*-diethyl-4-nitroaniline, 4-nitroaniline and pyridine-*N*-oxide, respectively, to the different eutectic mixtures (ca. 500  $\mu$ L).<sup>26,27</sup> Mixtures were then stirred (Eppendorf Thermomixer Comfort) at 323.15 K and 1400 rpm during 30 min, until complete dissolution. Regarding  $\pi^*$  and  $\beta$ , the longest wavelength absorption band was analyzed using UV-Vis spectroscopy (BioTeck Synergy HT microplate reader) at 323.15 K. The  $\alpha$  parameter was determined by <sup>13</sup>C nuclear magnetic resonance (NMR) spectra, using a Bruker Avance 300 equipment operating at 75 MHz. Deuterium oxide (D<sub>2</sub>O) was used as solvent and trimethylsilyl propanoic acid (TSP) as internal reference. At least three independent measurements were performed for each parameter and mixture.

#### *Mutual Solubilities*

The solubility of water in the eutectic mixtures was evaluated using a Metrohm 831 Karl Fischer, whereas the solubility of thymol in the water-rich phase was measured using a methodology previously detailed elsewhere.<sup>8,28</sup>

### **Theoretical Framework**

#### *Solid-Liquid Equilibria*

Considering that the solid phases crystallize independently as pure solids, and neglecting the effect of temperature on the heat capacities, the solubility of a solid in a liquid solvent can be described using the following expression:<sup>29</sup>

$$\ln(x_i \gamma_i^l) = \frac{\Delta_m H}{R} \left( \frac{1}{T_m} - \frac{1}{T} \right) + \frac{\Delta_m C_p}{R} \left( \frac{T}{T_m} - \ln \frac{T}{T_m} - 1 \right) \quad (1)$$

where  $\gamma_i^l$  is the activity coefficient of compound  $i$  in the liquid phase at a certain mole fraction composition  $x_i$ ,  $T$  is the absolute temperature,  $T_m$  and  $\Delta_m H$  are the melting temperature and enthalpy of the pure solute, respectively,  $R$  is the universal gas constant, and  $\Delta_m C_p$  is the difference between the heat capacity of compound  $i$  in the liquid and the solid states. Usually, the last term of equation 1 has a negligible value when compared with the first, especially for small differences between  $T$  and  $T_m$ , and thus it was not taken into account on this work.<sup>30,31</sup>

If an ideal liquid phase is assumed, the activity coefficients are equal to unity ( $\gamma_i^l = 1$ ), and the solubility curves can be easily obtained from Equation 1 as function of the temperature and the melting properties of the pure compounds. On the other hand, considering a non-ideal behavior, experimental activity coefficients can be obtained from Equation 1 using the experimental  $T$  data (solubility at given temperatures). The liquidus lines can, in this case, be obtained through Equation 1 but with the activity coefficients calculated through an appropriate activity coefficient model or EoS. In this work, PC-SAFT was used to model the phase diagrams, where the activity coefficients are obtained as the ratio between the fugacity coefficient of the solute in the liquid mixture and that of the pure compounds, both obtained from the system's residual Helmholtz energy calculated within the framework of the EoS.

#### *PC-SAFT EoS*

Due to the increasing complexity of the systems of interest in the chemical industry, there is a demand for broader and accurate thermodynamic models. Although cubic EoS are still the standard and proven methods for many applications,<sup>32</sup> they have known limitations when modelling the thermodynamic behavior and phase equilibria of complex systems like DES, that might present strong and short-range hydrogen-bonding interactions between their constituents. So far, molecular-based EoS with a strong theoretical background derived from statistical mechanics emerge as one of the

1  
2  
3 most promising alternatives to tackle these challenges.<sup>23,33–35</sup> These molecular-based  
4 EoS can explicitly account for different structural and energetic effects on the  
5 thermodynamic properties and phase equilibria of a system. The foremost application  
6 of such concept is the Statistical Associating Fluid Theory (SAFT) proposed by Chapman  
7 and co-workers in the late 80's<sup>36–39</sup> based on Wertheim's first order thermodynamic  
8 perturbation theory,<sup>40–43</sup> where a hard-sphere reference fluid is perturbed by distinct  
9 contributions reckoning particular effects such as the molecular shape, dispersive  
10 interactions and the hydrogen-bonding phenomenon. In the framework of SAFT,  
11 molecules were viewed as associating chains consisting of equally-sized spherical  
12 segments bonded tangentially, that may contain short-range associative sites.  
13  
14  
15  
16  
17  
18  
19  
20

21 Following the work of Chapman and co-workers, several SAFT-type equations have  
22 been proposed over the years mostly differing in the chosen reference term. One of  
23 the most fruitful modifications is PC-SAFT,<sup>20</sup> which considers a hard chain of freely-  
24 jointed hard spheres as a reference fluid (instead of a hard sphere). In the original  
25 publications,<sup>20,44</sup> PC-SAFT was demonstrated to perform better than the original model  
26 in several cases, especially for long-chain molecules. Moreover, it has already been  
27 successfully applied to eutectic mixtures.<sup>23,34,45,46</sup> The model equations are available in  
28 SI as well as the detailed procedure applied to obtain the PC-SAFT pure component  
29 parameters.  
30  
31  
32  
33  
34  
35  
36  
37

## 38 **Results and Discussion**

### 39 *Solid-liquid phase diagrams*

40  
41  
42  
43 The solid-liquid phase diagrams measured for the mixtures studied in this work are  
44 illustrated in Figures 1, 2 and S3, while the detailed data are listed in Tables S1 and S2  
45 of the Supporting Information. These systems exhibit a phase behavior characterized  
46 by a single eutectic point and, although the melting point depressions are relatively  
47 small and close to those predicted assuming an ideal liquid phase, in many cases it  
48 allows the formation of liquid mixtures at room temperature, while both pure  
49 compounds are solid.  
50  
51  
52  
53  
54  
55  
56  
57  
58  
59  
60

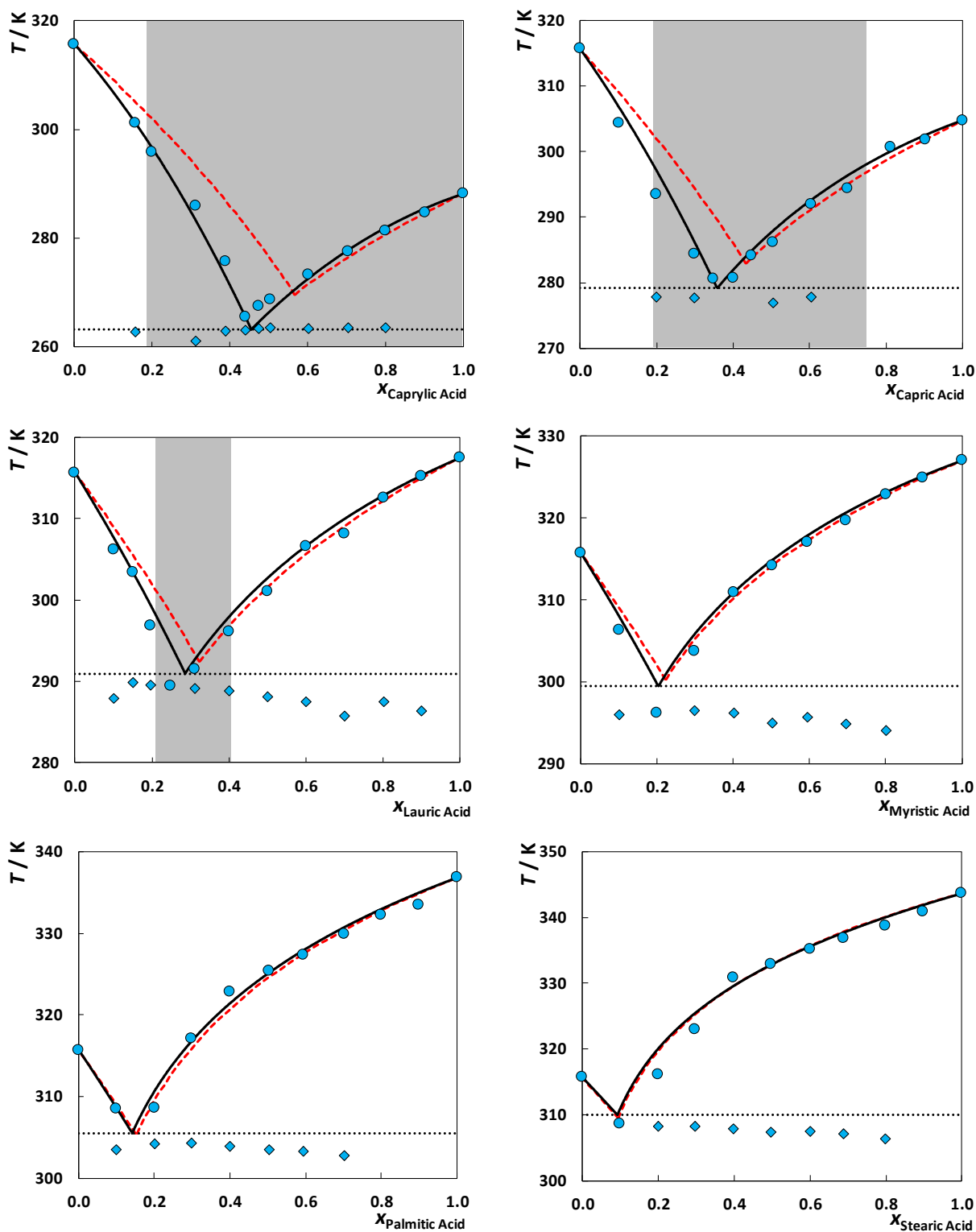
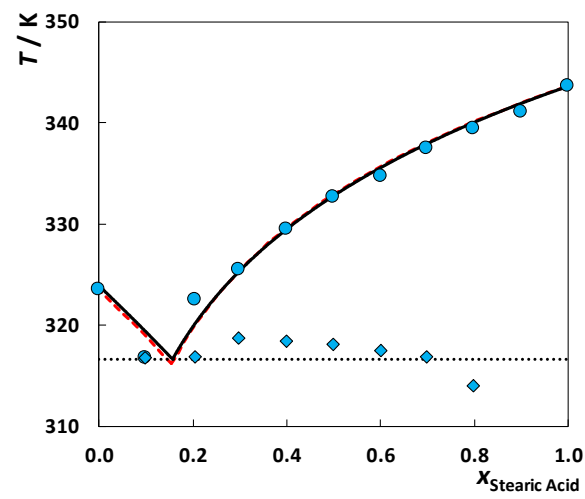
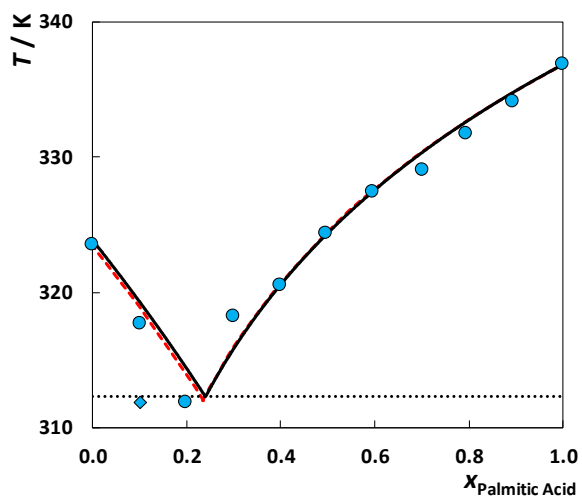
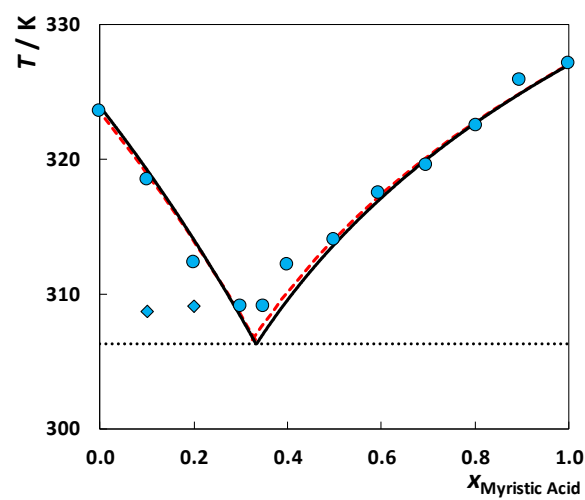
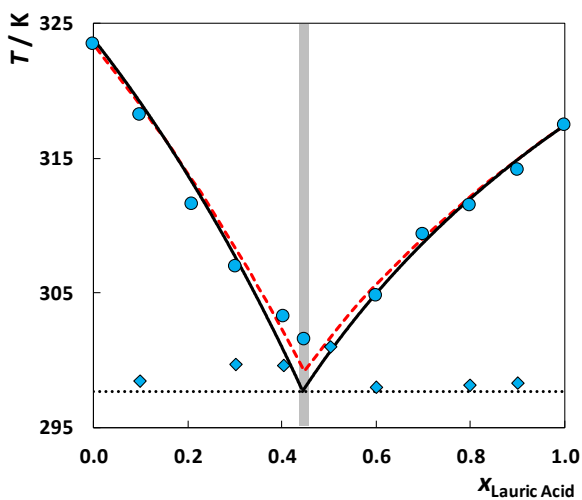
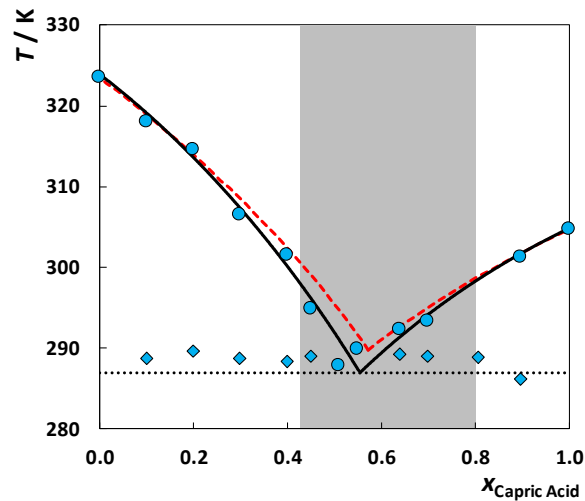
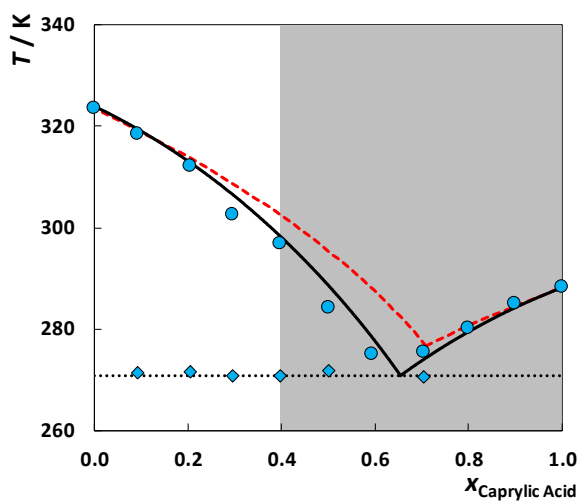


**Figure 1.** Solid-liquid phase diagrams of mixtures composed of monocarboxylic acids and *l*(-)-menthol. Symbols represent experimental data measured in this work while lines represent the modelling results: --, Ideal; —, PC-SAFT; ···,  $T^E$  predicted by PC-SAFT.

Gray regions represent the concentration range for which the mixture is liquid at room temperature ( $T = 298.15$  K).



1  
2  
3 **Figure 2.** Solid-liquid phase diagrams of mixtures composed of monocarboxylic acids  
4 and thymol. Symbols represent experimental data measured in this work while lines  
5 represent the modelling results: - -, Ideal; —, PC-SAFT; ····,  $T^E$  predicted by PC-SAFT.  
6 Gray regions represent the concentration range for which the mixture is liquid at room  
7 temperature ( $T = 298.15$  K).  
8  
9

10  
11  
12 The SLE phase diagram was described using two methodologies: i) assuming an ideal  
13 liquid phase ( $\gamma_i^l = 1$ ) and ii) calculating the activity coefficients through the associative  
14 PC-SAFT EoS. The modelling results are displayed in Figures 1 and 2 along with the  
15 experimental data. Moreover, the activity coefficients of each compound in the liquid  
16 phase obtained from PC-SAFT are displayed in Figures S4 and S5 of the SI, and their  
17 experimental values (accessed from the solubility data through Equation 1) reported in  
18 Tables S1 and S2.  
19  
20  
21  
22  
23  
24  
25

26 The quasi-ideal behavior observed for these mixtures suggests that the hydrogen-  
27 bonding (HB) networks established in these mixtures are not significantly different in  
28 intensity to those present in the pure compounds.<sup>23,47</sup> Even if the systems under study  
29 are quasi-ideal, the terpene solubility curves show small negative deviations from the  
30 ideal behavior, decreasing with the acid's chain length increase. While for caprylic and  
31 capric acids the eutectic temperature deviates approximately 10 K from ideal behavior,  
32 for stearic acid these are essentially identical. These deviations from ideality suggest  
33 the existence of interactions between the terpene and the short chain acid slightly  
34 stronger than those observed in the pure terpenes. The decrease of the non-ideality  
35 with the acid's chain length is probably due to an increase of the dispersive  
36 interactions that eventually become dominant on these systems with very long alkyl  
37 chains.  
38  
39  
40  
41  
42  
43  
44  
45  
46

47  
48 Figures 1 and 2 show that PC-SAFT can adequately correlate the SLE experimental data  
49 of mixtures involving thymol or  $\iota(-)$ -menthol, and monocarboxylic acids. For the  
50 systems containing thymol, the PC-SAFT predictions using solely the pure-component  
51 parameters fitted to the pure liquid densities and vapor pressures were found to  
52 provide a very good description of the experimental data. On the other hand, for the  
53 systems with  $\iota(-)$ -menthol a binary interaction parameter increasing the cross-  
54  
55  
56  
57  
58  
59  
60

1  
2  
3 association interactions between  $\iota(-)$ -menthol and the acids was required. These  
4 binary interaction parameters, listed in Table S3, were obtained through the  
5 minimization of the temperature ( $T$ ) average absolute deviation (AAD/K) expressed as:  
6  
7

$$AAD / K = \frac{1}{N} \sum_{i=1}^N |T_i^{calc}(K) - T_i^{exp}(K)| \quad (2)$$

8  
9  
10  
11  
12  
13 where  $T_i^{calc}$  and  $T_i^{exp}$  are the calculated and the experimental melting temperatures,  
14 respectively. The need for a binary interaction parameter to accurately describe quasi-  
15 ideal systems may seem surprising, but it might be related to an asymmetry present in  
16 these systems. It can be observed that the acid solubility curve displays an almost ideal  
17 behavior, or presents slight positive deviations from ideality, conversely to what is  
18 observed in the terpene solubility curves. These unsymmetrical small deviations from  
19 ideality is difficult to be captured by most thermodynamic models, as discussed in our  
20 previous work.<sup>34</sup> Still, the low magnitude of the deviations from ideality (even in the  
21 systems involving  $\iota(-)$ -menthol) allowed to correlate the binary interaction parameter  
22 between  $\iota(-)$ -menthol and the carboxylic acids, with the molecular weight of the acid:  
23  
24  
25  
26  
27  
28  
29

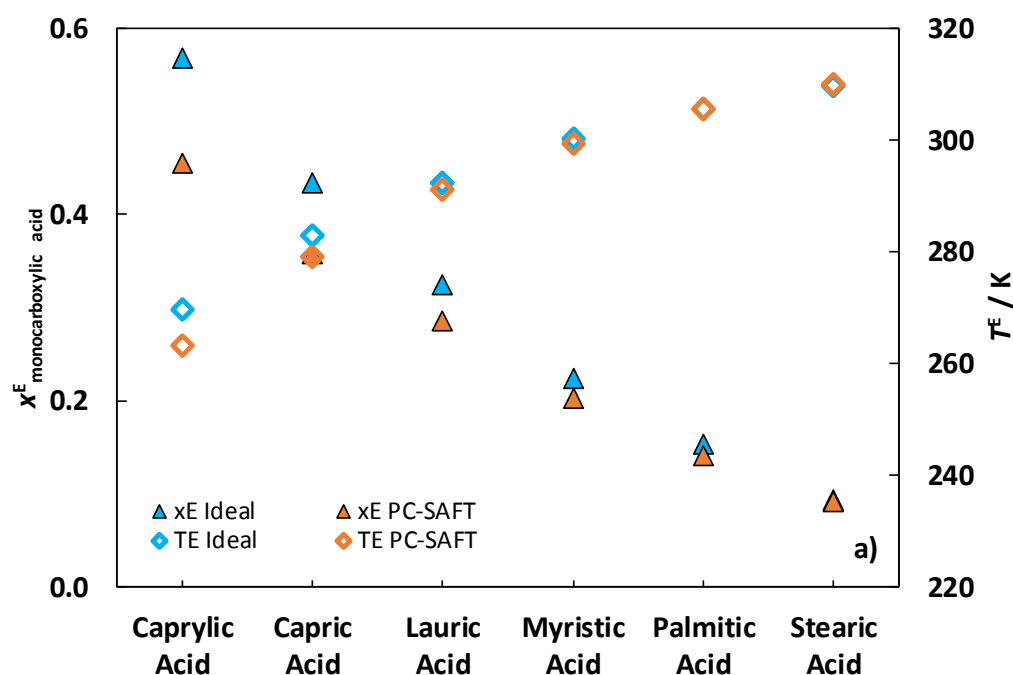
$$k_{ij\_eps} = 0.0004837 \times M_w(g/mol) - 0.1336, R^2 = 0.9586 \quad (3)$$

30  
31  
32  
33  
34  
35 As can be seen from Equation 3, the absolute values of  $k_{ij\_eps}$  estimated in the mixtures  
36 with  $\iota(-)$ -menthol decrease with an increase of the acid's chain length as previously  
37 observed in eutectic mixtures composed of  $[N_{xxx}]Cl$  + monocarboxylic acids.<sup>23</sup>  
38  
39  
40

41 The average absolute deviations assuming ideality or using PC-SAFT are reported in  
42 Table S3. PC-SAFT EoS decreases the AAD relatively to the ideality results for most  
43 systems, especially in those exhibiting negative deviations from the ideal behavior in  
44 the terpene solubility curve. This stresses the advantage of using EoS able to explicitly  
45 account for hydrogen-bonding interactions, and emphasizes the usefulness of PC-SAFT  
46 to describe the thermodynamic behavior of eutectic mixtures and DES.  
47  
48  
49  
50

51  
52 Since PC-SAFT was able to accurately describe the experimental solubility curves of  
53 mixtures of terpenes and monocarboxylic acids, it was used to provide estimates of  
54 their eutectic points. These are shown in Figure 3 and detailed in Table S4.  
55  
56  
57

As depicted in Figures 1 and 2, in some cases eutectic composition predicted by PC-SAFT is somewhat different from that predicted assuming ideality. This difference is smaller for mixtures with thymol than for mixtures with L(-)-menthol. For both sets (thymol + monocarboxylic acids and L(-)-menthol + monocarboxylic acids) phase diagrams, the eutectic temperature was observed to regularly increase with the acids molecular weight – as shown in Figures 3 and S3. The mole fraction of carboxylic acid at the eutectic composition, on the opposite, decreases with increasing acid molecular weight. Moreover, a fixed stoichiometric relationship between the hydrogen bond donor and acceptor cannot be observed. Instead a continuous change with the acid chain length can be observed in Figure 3, stressing the highly tunable character of the eutectic point of these mixtures and the wide concentration range to formulate these eutectic solvents as highlighted in Figures 1 and 2.



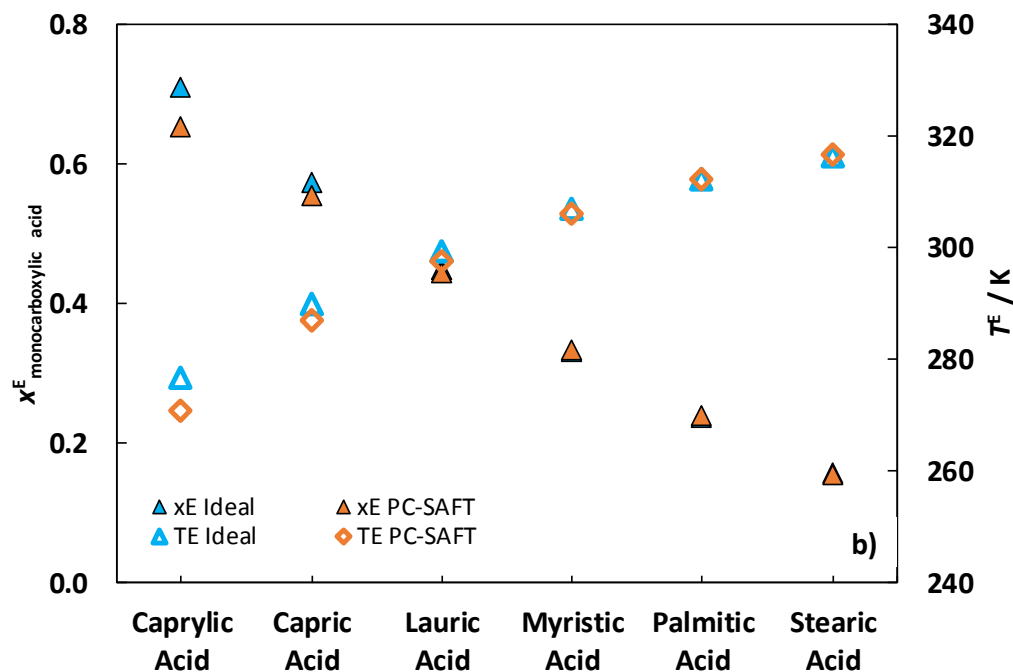


**Figure 3.** Eutectic compositions and temperatures of the systems involving a) L(-)-menthol and b) thymol.

In Figure S6 the SLE behavior of lauric acid with the terpenes (L(-)-menthol and thymol) is depicted. The results show that the change in the terpene used has no influence on the qualitative behavior of the acid's solubility curve. However, the different melting properties of thymol and L(-)-menthol, and the possibility of cross-association with acid molecules, are found to considerably influence the terpene solubility curve resulting in different eutectic points, both in temperature and composition; as correctly described by the PC-SAFT EoS.

For comparison purposes few information has been found, that also supports the importance of modeling tasks: Ribeiro et al.<sup>17</sup> reported 286.99 K as the melting point of the mixture DL-menthol and lauric acid at 0.66:0.33 (mole fraction ratio). In this work, the values measured (at nearby compositions) were: 291.54 K at the composition ratio 0.69:0.31 and 296.17 K at the composition ratio 0.60:0.40. The value predicted using PC-SAFT EoS at the exact composition ratio 0.66:0.33 is 293.97 K. Moreover, the eutectic temperature predicted by PC-SAFT was 290.97 K at 0.71:0.29.

1  
2  
3 In order to evaluate the systems involving thymol + monocarboxylic acid and L(-)-  
4 menthol + monocarboxylic acid as potential solvents, their mixtures with compositions  
5 close to the eutectic point are characterized in the next sections. Density and viscosity  
6 are relevant solvent properties since they have an important impact on mass transport  
7 phenomena, affecting solvents suitability for specific applications, while the  
8 solvatochromic parameters help to define the mixtures polarity, aiming at better  
9 understand the influence of the components chemical structure on their properties,  
10 for a priori design of eutectic mixtures.  
11  
12  
13  
14  
15

### 16 *Densities*

17  
18  
19  
20 Densities of the eutectic mixtures were determined at atmospheric pressure, in the  
21 temperature range between 278.15 and 373.15 K, and are reported in Figure S7 and  
22 Tables S5 and S6 of the SI, along with the mole fraction of the monocarboxylic acid.  
23 The densities of pure thymol and L(-)-menthol<sup>48</sup> are also displayed in Figure S7 for  
24 comparative purposes.  
25  
26  
27  
28  
29

30 While all mixtures studied are less dense than water, eutectic mixtures with thymol  
31 present higher densities than those with L(-)-menthol, and their range of variation is  
32 also broader. The densities of the eutectic mixtures of monocarboxylic acids with L(-)-  
33 menthol decrease with increasing alkyl chain of the monocarboxylic acid. Concerning  
34 the mixtures with thymol, the opposite trend is observed, i.e. the densities decrease  
35 with decreasing chain length of the monocarboxylic acid. This is explained by the fact  
36 that the density of pure thymol is higher than the correspondent mixtures with the  
37 monocarboxylic acids, while the density of pure L(-)-menthol is in between those with  
38 the acids – Figure S7. Thus, and taking into account that at the eutectic point when  
39 increasing the alkyl chain length of the fatty acid the molar fraction of terpene  
40 increases, by adding thymol the mixtures densities tend to increase while adding L(-)-  
41 menthol densities have a tendency to decrease.  
42  
43  
44  
45  
46  
47  
48  
49  
50

51 Since the SLE of the different systems analyzed was successfully described using the  
52 PC-SAFT EoS, the ability of this model to predict the densities of these systems was  
53 also investigated. The results are presented in Figure S7 and the AAD to the  
54  
55  
56  
57  
58  
59  
60

1  
2  
3 experimental densities are presented in Table S7. The deviations obtained range  
4 between 0.02 and 1.35% with an average value (for all 183 data points) of 0.46%.  
5  
6

7 The excess molar volumes,  $V_m^E$ , were calculated<sup>49</sup> through the experimental density  
8 data measured in this work (Table S5 and S6) and are depicted in Figure S8. The  
9 densities of pure thymol,  $\iota$ (-)-menthol and monocarboxylic acids were taken from  
10 literature.<sup>48,50,51</sup>  $V_m^E$  are in general close to zero, reinforcing the ideal character of  
11 these mixtures. Mixtures involving  $\iota$ (-)-menthol present mainly negative excess molar  
12 volumes while the opposite is observed for thymol. Almost no dependence with  
13 temperature is observed. Since the excess molar volumes are negligible, the molar  
14 volume of the mixture can be directly calculated through the densities of the pure  
15 components.<sup>52</sup> The average absolute deviation are 0.21 and 0.27  $\text{cm}^3\cdot\text{mol}^{-1}$  for  
16 mixtures involving  $\iota$ (-)-menthol and thymol, respectively.  
17  
18  
19  
20  
21  
22  
23  
24

25 Additionally, a study on the isobaric thermal expansion coefficients,  $\alpha_p$ , was performed  
26 and is presented in SI. The derived  $\alpha_p$  values are in general very similar, varying  
27 between  $-8.5 \times 10^{-4}$  and  $-8.9 \times 10^{-4}$ . No well-defined dependence of  $\alpha_p$  with the chain  
28 length of the monocarboxylic acid was observed within the uncertainty of the  
29 experimental data. Moreover, the  $\alpha_p$  of eutectic mixtures containing either caprylic,  
30 palmitic or stearic acids varies significantly with the selected terpene. With the  
31 exception of caprylic acid, the isobaric thermal expansion coefficients are higher in the  
32 eutectic mixtures with thymol than in those containing  $\iota$ (-)-menthol. Regarding the  $\alpha_p$   
33 values predicted using PC-SAFT, they increase with the chain length of the  
34 monocarboxylic acid. Moreover, no significant difference is observed when using  
35 thymol or  $\iota$ (-)-menthol. Experimental and calculated  $\alpha_p$  values present significant  
36 differences in mixtures involving the caprylic and capric acids, but they also suggest  
37 that the  $\alpha_p$  values decrease for the eutectic mixtures of acids above myristic.  
38  
39  
40  
41  
42  
43  
44  
45  
46  
47  
48

#### 49 *Viscosities*

50  
51  
52 Viscosity data for the eutectic mixtures under study were also measured at  
53 atmospheric pressure in the temperature range between 278.15 and 373.15 K, which  
54 are depicted in Figure S9 and detailed in Tables S8 and S9. For comparative purposes  
55  
56  
57  
58  
59  
60

1  
2  
3 the viscosities of pure thymol and L(-)-menthol were also measured and are shown in  
4 Figure S9 (and Tables S8 and S9).  
5

6  
7 The viscosity values are fairly low for this type of solvents, and are observed to  
8 increase with the acid chain length. However, the effect of chain length is much less  
9 relevant at higher temperatures where viscosity values are very similar. Contrary to  
10 what is observed for the densities, the range of viscosities of eutectic mixtures of L(-)-  
11 menthol is broader than the range of viscosities of eutectic mixtures involving thymol,  
12 and thymol-based eutectic mixtures are significantly less viscous.  
13  
14  
15  
16  
17

18  
19 A comparison between the viscosity of pure compounds and their mixtures is  
20 displayed in Figure S10. The viscosities of pure monocarboxylic acids were taken from  
21 literature.<sup>50,51</sup> In most cases the viscosity of the mixtures is in between (or higher) the  
22 viscosities of the pure components. There are only two conditions where the viscosity  
23 of the mixture is lower than the viscosity of both pure components: L(-)-menthol +  
24 lauric acid at 333.15 K and L(-)-menthol + myristic acid at 328.15 K. For caprylic and  
25 capric acids, their pure viscosities are generally lower than the viscosities of their  
26 mixtures with terpenes. For heavier acids, viscosities of the pure compounds are  
27 higher than those for mixtures with terpenes. Regarding L(-)-menthol, the viscosity of  
28 the pure terpene is higher than the viscosity of the mixture involving monocarboxylic  
29 acids with chain lengths from C8 to C14, when the viscosity of the pure terpene  
30 becomes lower. The viscosity of pure thymol is only higher in the system involving  
31 caprylic acid. Additionally, the viscosity ideal mixture rule<sup>49</sup> ( $\ln \eta_{mix} = x_1 \ln \eta_1 +$   
32  $x_2 \ln \eta_2$ ) was applied and proved to correctly describe the experimental data. The  
33 average absolute deviation between the predicted (by the viscosity ideal mixture rule)  
34 and the experimental was of 0.19 and 0.28 mPa·s for mixtures involving L(-)-menthol  
35 and thymol, respectively.  
36  
37  
38  
39  
40  
41  
42  
43  
44  
45  
46  
47  
48

49 The energy barrier ( $E$ ), i.e., the energy value that must be overcome in order for the  
50 molecules to move past each other<sup>53</sup> was also investigated (study available on SI).  $E$  is  
51 observed to be lower for the thymol eutectic mixtures and to increase with the chain  
52 length of the monocarboxylic acid used in the mixture. The addition of monocarboxylic  
53  
54  
55  
56  
57  
58  
59  
60

1  
2  
3 acids decreases the energy barrier, being this decrease more pronounced when using  
4 thymol and small monocarboxylic acids.  
5

#### 6 7 *Kamlet Taft Solvatochromic Parameters* 8

9  
10 The Kamlet Taft parameters were measured at 323.15 K and are presented in Figure 4  
11 and Table S10 (equations available in SI). The solvatochromic  $\pi^*$  is related with the  
12 polarizability/dipolarity of the mixture. This is higher for mixtures involving thymol due  
13 to the presence of the aromatic ring in the structure. Although it is not available for  
14 pure thymol, due to its higher melting point, it is expected to be larger than for L(-)-  
15 menthol. Moreover, there is an almost linear increase with the number of carbons of  
16 the alkyl chain length of the monocarboxylic acid, which is probably connected to the  
17 simultaneous increase of the thymol mole fraction at eutectic. The  $\pi^*$  for the L(-)-  
18 menthol based eutectic solvents does not vary with the acid used, presenting an  
19 almost constant value, close to the value of pure L(-)-menthol.  
20  
21  
22  
23  
24  
25  
26

27  
28 The  $\beta$  and  $\alpha$  parameters describe the hydrogen bond acceptor and donor capacity,  
29 respectively. The variation observed on parameter  $\beta$  are the opposite of those  
30 discussed for parameter  $\pi^*$ : L(-)-menthol presents higher values than thymol, and  
31 increases linearly with the number of carbons of the monocarboxylic acid, while for  
32 mixtures with thymol, this value is practically constant, and very close to zero. This is  
33 related to the aromatic nature of the ring on thymol that substantially reduced its  
34 ability to act as a hydrogen bonding acceptor. The capacity to act as hydrogen bond  
35 donor is higher in mixtures with thymol, being almost independent on the alkyl chain  
36 length of the acid, while in mixtures containing L(-)-menthol  $\alpha$  decreases linearly with  
37 the number of carbons of the alkyl chain of the acid, on a trend that evolves towards  
38 the value of the pure L(-)-menthol.  
39  
40  
41  
42  
43  
44  
45  
46

47  
48 In order to evaluate the consistency of these results, the sigma profiles of thymol and  
49 L(-)-menthol were computed by COSMO-RS and are presented in Figure S11. These  
50 profiles suggest that L(-)-menthol has a larger capacity to accept hydrogen bonds and  
51 thus should have a higher  $\beta$ , while thymol has a bigger capacity to donate H-bonds,  
52 and thus should present a higher  $\alpha$ . Moreover, the addition of non-polar groups to the  
53  
54  
55  
56  
57

monocarboxylic acid, that do not have the capacity to form hydrogen bonding, leads to the decrease of  $\alpha$  and increase of  $\beta$ , as observed for  $\iota(-)$ -menthol.

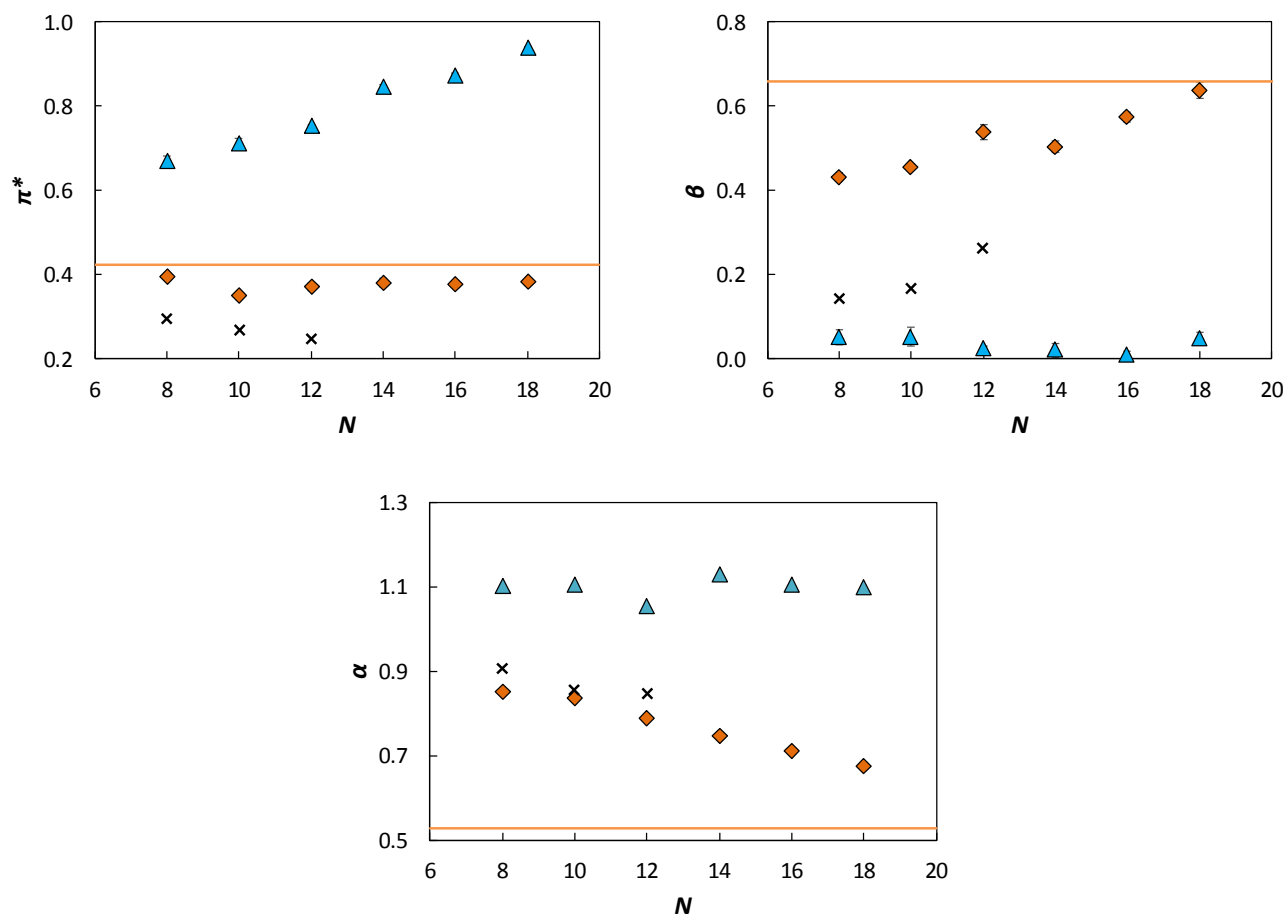


**Figure 4.** Kamlet-Taft solvatochromic parameters of the different pure compounds and mixtures studied at 323.15 K, as a function of the number of carbons of the monocarboxylic acid. Legend:  $\blacktriangle$ , thymol + monocarboxylic acid,  $\blacklozenge$ ,  $\iota(-)$ -menthol + monocarboxylic acid,  $-$ , pure  $\iota(-)$ -menthol,  $\times$ , pure monocarboxylic acids.

Florindo et al.<sup>54</sup> measured the Kamlet-Taft solvatochromic parameters of mixtures of  $\iota(-)$ -menthol with caprylic ( $\beta = 0.43/0.50$ <sup>54</sup>,  $\pi^* = 0.39/0.41$ <sup>54</sup>,  $\alpha = 0.85/1.77$ <sup>54</sup>) and lauric ( $\beta = 0.54/0.57$ <sup>54</sup>,  $\pi^* = 0.37/0.37$ <sup>54</sup>,  $\alpha = 0.79/1.79$ <sup>54</sup>) acids. The only parameter that presents significant differences between the two sets of experimental data is the hydrogen-bond donor acidity,  $\alpha$ . This was obtained using different probes and

1  
2  
3 different methodologies what can be reason for the differences observed, once the  
4 solvatochromic parameters are probe dependent.  
5

6  
7 To evaluate the potential of these mixtures as solvents, comparisons with other  
8 molecular solvents are discussed. The Kamlet-Taft solvatochromic parameters of some  
9 common solvents are displayed in Table S10. In general, mixtures involving thymol  
10 display a higher ability to establish non-specific interactions with a solute than organic  
11 solvents, as supported by the higher value of  $\pi^*$ . On the other hand, these thymol-  
12 based mixtures present higher hydrogen-bond acidity values than alcohols, ketones,  
13 alkanes, aromatics and the pure acids, and slightly lower values than water. Regarding  
14 the ability to accept protons, mixtures involving L(-)-menthol present similar values to  
15 water and other organic solvents while the mixtures involving thymol present values  
16 close to zero like hydrocarbons, meaning no ability to accept protons.  
17  
18  
19  
20  
21  
22  
23  
24

25 To assess the hydrophobicity of the studied systems, quantitative studies on the  
26 mutual solubilities of the investigated mixtures (with compositions close to the  
27 eutectic point – Tables S5 and S6) with water were performed at 298.15 K and the  
28 results are presented in Figure 5 and Table S11. The solubility of the L(-)-menthol in  
29 water was not measured since this compound was not possible to quantify using the  
30 analytical technique adopted. As shown in Figure 5, the solubility of water in the  
31 eutectic mixtures decreases with the increase of the alkyl chain length of the acid, i.e.  
32 the hydrophobicity of the HBD. The same trend is observed for the solubility of thymol  
33 (+ monocarboxylic acids) in water. When comparing with the solubility of pure thymol  
34 in water at 298.15 K ( $x_{\text{thymol}} = 11.8 \times 10^{-5}$ )<sup>8</sup> it is possible to conclude that the presence  
35 of the acid in the mixture decreases the solubility of the terpene in more than one  
36 order of magnitude. The solubilities of the pure acids in water vary from  $x_{\text{caprylic acid}} =$   
37  $9.88 \times 10^{-5}$  ( $T = 303.15$  K) to  $x_{\text{stearic acid}} = 3.79 \times 10^{-8}$  ( $T = 298.15$  K).<sup>55</sup>  
38  
39  
40  
41  
42  
43  
44  
45  
46  
47  
48

49 Additionally, the systems investigated were mixed with water (in exactly the same  
50 masses – 500  $\mu\text{L}$  each) in the presence of dyes. Results are presented in Figure 6 that  
51 shows a separation between the organic and aqueous phases. Rhodamine 6G,  
52 presenting a non-polar character seems to be completely extracted into the  
53 hydrophobic organic phase (pink-dyed phase), terpene + monocarboxylic acid. By the  
54  
55  
56  
57  
58  
59  
60

other hand the Brilliant Blue FCF (E133) migrates into the water phase (blue-dyed phase).

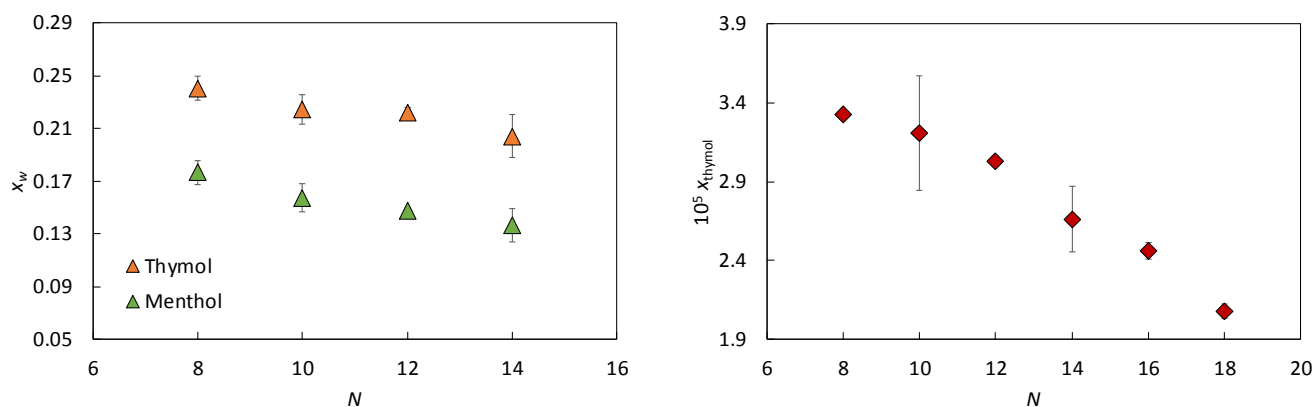


**Figure 5.** Solubility of water in the eutectic mixtures,  $x_w$ , and solubility of thymol (+ monocarboxylic acids),  $x_{\text{thymol}}$ , in water at 298.15 K and as a function of the number of carbons of the alkyl chain length of the monocarboxylic acid,  $N$ .

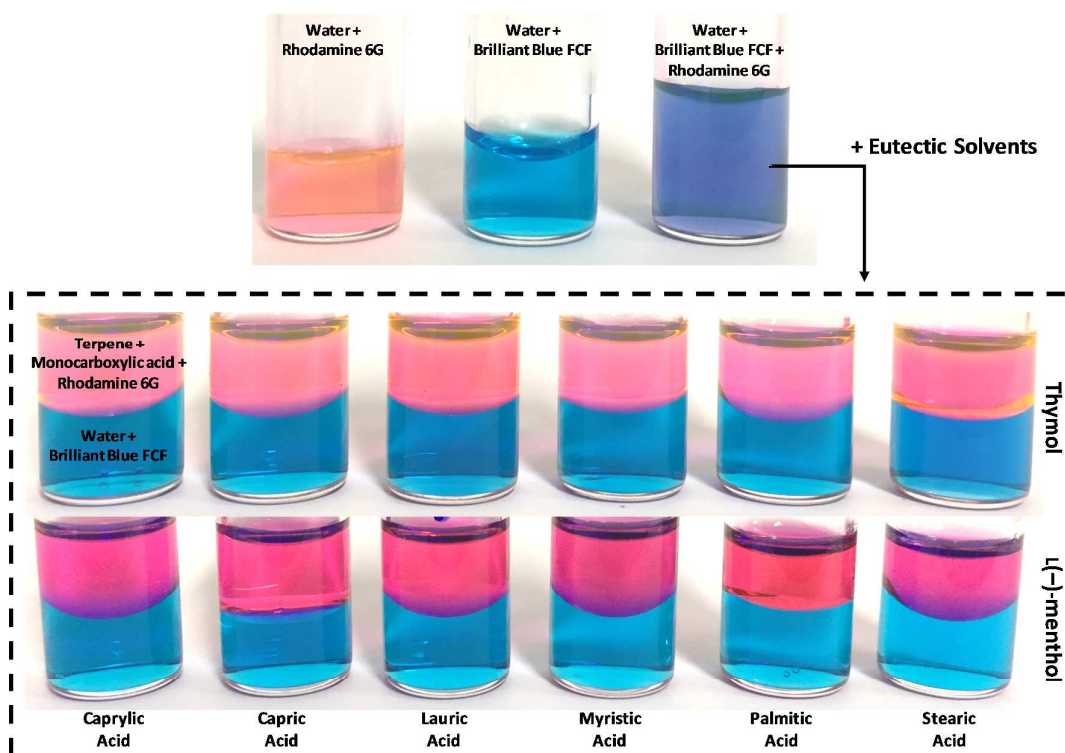


**Figure 6.** Mixture of the solvents investigated in this work with water and the dyes Rhodamine 6G and Brilliant Blue FCF.

1  
2  
3 In summary, we investigated mixtures involving terpenes and monocarboxylic acids  
4 aiming to characterize and design these solvents. The SLE phase diagrams of the  
5 mixtures were measured in the whole composition range using DSC, and showed a  
6 broader composition range in the liquid state, at room temperature than previously  
7 admitted. Generally the systems exhibited small deviations from ideality and a eutectic  
8 point close to that predicted assuming ideality. Therefore, although often labeled as  
9 DES, these systems do not present negative deviations large enough to induce a  
10 significant melting point depression. However, it must be stressed that room  
11 temperature solvents can be obtained for many of these mixtures on a wide  
12 composition range and not fixed to any particular stoichiometric relationship between  
13 the hydrogen bond donor and acceptor, even at the eutectic point, what reinforces the  
14 tunable character of the liquid phase region of these mixtures. The experimental solid-  
15 liquid phase diagrams were successfully described using the PC-SAFT EoS, which  
16 provided reliable estimates of the eutectic points and of the solvents densities. This  
17 EoS also showed that liquid phases are quasi-ideal. The eutectic mixtures present  
18 densities lower than water and low viscosities (1.3 – 50.6 mPa·s) and in general  
19 eutectic mixtures containing thymol were less viscous but more dense than those with  
20  $\iota$ (-)-menthol. A series of solvatochromic parameters were measured in order to  
21 address the polarity of the mixtures investigated. All the parameters are strongly  
22 influenced by the terpene used and in some cases vary with the alkyl chain length of  
23 the monocarboxylic acid. Mixtures involving thymol present a higher hydrogen-bond  
24 acidity character, as well as higher nonspecific interactions.  $\iota$ (-)-menthol presents a  
25 higher hydrogen-bond basicity character and a slight increase of this parameter with  
26 the increase of the alkyl chain of the monocarboxylic acid. Moreover, the mixtures  
27 reported here displays a high capacity to donate (thymol-based mixtures) and accept  
28 ( $\iota$ (-)-menthol based mixtures) protons when compared to some organic molecular  
29 solvents and very close to water. The polarity dependence on the alkyl chain length of  
30 the monocarboxylic acid favors the design of new solvents. The measured mutual  
31 solubilities with water prove the hydrophobic character of the mixtures investigated.

## 32 33 34 35 36 37 38 39 40 41 42 43 44 45 46 47 48 49 50 51 52 53 54 **Acknowledgements** 55 56 57 58 59 60

1  
2  
3 This work was developed in the scope of the project CICECO – Aveiro Institute of  
4 Materials, POCI-01-0145-FEDER-007679 (Ref. FCT UID/CTM/50011/2013) and  
5 Associate Laboratory LSRE-LCM, POCI-01-0145-FEDER-006984 (Ref. FCT  
6 UID/EQU/50020/2013), both financed by national funds through the FCT/MEC and  
7 when appropriate co-financed by FEDER under the PT2020 Partnership Agreement.  
8 This work is also a result of project “AIProcMat@N2020 - Advanced Industrial  
9 Processes and Materials for a Sustainable Northern Region of Portugal 2020”, with the  
10 reference NORTE-01-0145-FEDER-000006, supported by Norte Portugal Regional  
11 Operational Programme (NORTE 2020), under the Portugal 2020 Partnership  
12 Agreement, through the European Regional Development Fund (ERDF). M.A.R.M  
13 acknowledges FCT for her PhD grant (SFRH/BD/87084/2012). FCT is also acknowledged  
14 for funding the project DeepBiorefinery (PTDC/AGRTEC/1191/2014). P.V.A.P. and  
15 G.J.M. thank the national funding agencies CNPq (National Council for Scientific and  
16 Technological Development) (305870/2014-9, 309780/2014-4, 140702/2017-2,  
17 406918/2016-3, 406963/2016-9), FAPESP (Research Support Foundation of the State  
18 of Sao Paulo) (2014/21252-0, 2016/08566-1), FAEPEX/UNICAMP (Fund for Research,  
19 Teaching, and Extension) (0125/16) and CAPES (Coordination of Improvement of  
20 Higher Level Personnel) for financial support and scholarships. E.A.C thanks FCT for the  
21 PhD grant SFRH/BD/130870/2017. Christoph Held acknowledges financial support  
22 from Max – Buchner Research Foundation and from German Science Foundation (DFG)  
23 HE 7165/7-1.

### Supporting Information

40  
41  
42 The Supporting Information is available free of charge on the ACS Publications website.

43  
44  
45 Structures of the investigated compounds; mixtures NMR; experimental and calculated  
46 solid-liquid phase diagrams and activity coefficients; densities, excess molar volumes  
47 and isobaric thermal expansion coefficients; viscosities and energy barrier; Kamlet Taft  
48 solvatochromic parameters; sigma profiles of pure compounds; mutual solubilities  
49 with water; PC-SAFT parameters, their description and calculation; ideal and predicted  
50 (PC-SAFT) eutectic points; densities, viscosities and KT solvatochromic parameters  
51 equations (PDF).

## References

- (1) Zhang, Q.; De Oliveira Vigier, K.; Royer, S.; Jérôme, F. Deep Eutectic Solvents: Syntheses, Properties and Applications. *Chem. Soc. Rev.* **2012**, *41* (21), 7108–7146, DOI 10.1039/c2cs35178a.
- (2) Florindo, C.; Oliveira, F. S.; Rebelo, L. P. N.; Fernandes, A. M.; Marrucho, I. M. Insights into the Synthesis and Properties of Deep Eutectic Solvents Based on Cholinium Chloride and Carboxylic Acids. *ACS Sustain. Chem. Eng.* **2014**, *2* (10), 2416–2425, DOI 10.1021/sc500439w.
- (3) Maugeri, Z.; Domínguez de María, P. Novel Choline-Chloride-Based Deep-Eutectic-Solvents with Renewable Hydrogen Bond Donors: Levulinic Acid and Sugar-Based Polyols. *RSC Adv.* **2012**, *2* (2), 421–425, DOI 10.1039/C1RA00630D.
- (4) van Osch, D. J. G. P.; Zubeir, L. F.; van den Bruinhorst, A.; Rocha, M. A. A.; Kroon, M. C. Hydrophobic Deep Eutectic Solvents as Water-Immiscible Extractants. *Green Chem.* **2015**, *17* (9), 4518–4521, DOI 10.1039/C5GC01451D.
- (5) Florindo, C.; Branco, L. C.; Marrucho, I. M. Development of Hydrophobic Deep Eutectic Solvents for Extraction of Pesticides from Aqueous Environments. *Fluid Phase Equilib.* **2017**, *448* (25), 135–142, DOI 10.1016/j.fluid.2017.04.002.
- (6) van Osch, D. J. G. P.; Parmentier, D.; Dietz, C. H. J. T.; van den Bruinhorst, A.; Tuinier, R.; Kroon, M. C. Removal of Alkali and Transition Metal Ions from Water with Hydrophobic Deep Eutectic Solvents. *Chem. Commun.* **2016**, *52* (80), 11987–11990, DOI 10.1039/C6CC06105B.
- (7) Tereshatov, E. E.; Boltoeva, M. Y.; Folden, C. M. First Evidence of Metal Transfer into Hydrophobic Deep Eutectic and Low-Transition-Temperature Mixtures: Indium Extraction from Hydrochloric and Oxalic Acids. *Green Chem.* **2016**, *18* (17), 4616–4622, DOI 10.1039/c5gc03080c.
- (8) Martins, M. A. R.; Silva, L. P.; Ferreira, O.; Schröder, B.; Coutinho, J. A. P.; Pinho, S. P. Terpenes Solubility in Water and Their Environmental Distribution. *J. Mol. Liq.* **2017**, *241*, 996–1002, DOI 10.1016/j.molliq.2017.06.099.
- (9) Shen, Q.; Li, X.; Li, W.; Zhao, X. Enhanced Intestinal Absorption of Daidzein by Borneol/Menthol Eutectic Mixture and Microemulsion. *AAPS PharmSciTech*

- 2011, 12 (4), 1044–1049, DOI 10.1208/s12249-011-9672-4.
- (10) Phaechamud, T.; Tuntarawongsa, S. Transformation of Eutectic Emulsion to Nanosuspension Fabricating with Solvent Evaporation and Ultrasonication Technique. *Int. J. Nanomedicine* **2016**, 11, 2855–2865, DOI 10.2147/IJN.S108355.
- (11) Mohammadi-Samani, S.; Yousefi, G.; Mohammadi, F.; Ahmadi, F. Meloxicam Transdermal Delivery: Effect of Eutectic Point on the Rate and Extent of Skin Permeation. *Iran. J. Basic Med. Sci.* **2014**, 17 (2), 112–118.
- (12) Stott, P. W.; Williams, A. C.; Barry, B. W. Transdermal Delivery from Eutectic Systems: Enhanced Permeation of a Model Drug, Ibuprofen. *J. Control. Release* **1998**, 50 (1), 297–308, DOI 10.1016/S0168-3659(97)00153-3.
- (13) Yong, C. S.; Jung, S. H.; Rhee, J.-D.; Choi, H.-G.; Lee, B.-J.; Kim, D.-C.; Choi, Y. W.; Kim, C.-K. Improved Solubility and In Vitro Dissolution of Ibuprofen from Poloxamer Gel Using Eutectic Mixture with Menthol. *Drug Deliv.* **2003**, 10 (3), 179–183, DOI 10.1080/713840406.
- (14) Kaplun-Frischoff, Y.; Touitou, E. Testosterone Skin Permeation Enhancement by Menthol through Formation of Eutectic with Drug and Interaction with Skin Lipids. *J. Pharm. Sci.* **1997**, 86 (12), 1394–1399, DOI 10.1021/js9701465.
- (15) Kang, L.; Jun, H. W.; McCall, J. W. Physicochemical Studies of Lidocaine-Menthol Binary Systems for Enhanced Membrane Transport. *Int. J. Pharm.* **2000**, 206 (1–2), 35–42, DOI 10.1016/S0378-5173(00)00505-6.
- (16) Nazzal, S.; Smalyukh, I. .; Lavrentovich, O. .; Khan, M. A. Preparation and in Vitro Characterization of a Eutectic Based Semisolid Self-Nanoemulsified Drug Delivery System (SNEDDS) of Ubiquinone: Mechanism and Progress of Emulsion Formation. *Int. J. Pharm.* **2002**, 235 (1), 247–265, DOI 10.1016/S0378-5173(02)00003-0.
- (17) Ribeiro, B. D.; Florindo, C.; Iff, L. C.; Coelho, M. A. Z.; Marrucho, I. M. Menthol-Based Eutectic Mixtures: Hydrophobic Low Viscosity Solvents. *ACS Sustain. Chem. Eng.* **2015**, 3 (10), 2469–2477, DOI 10.1021/acssuschemeng.5b00532.
- (18) Aroso, I. M.; Craveiro, R.; Rocha, Â.; Dionísio, M.; Barreiros, S.; Reis, R. L.; Paiva,

- 1  
2  
3 A.; Duarte, A. R. C. Design of Controlled Release Systems for THEDES—  
4 Therapeutic Deep Eutectic Solvents, Using Supercritical Fluid Technology. *Int. J.*  
5 *Pharm.* **2015**, *492* (1), 73–79, DOI 10.1016/j.ijpharm.2015.06.038.  
6  
7  
8 (19) Aroso, I. M.; Silva, J. C.; Mano, F.; Ferreira, A. S. D.; Dionísio, M.; Sá-Nogueira, I.;  
9 Barreiros, S.; Reis, R. L.; Paiva, A.; Duarte, A. R. C. Dissolution Enhancement of  
10 Active Pharmaceutical Ingredients by Therapeutic Deep Eutectic Systems. *Eur. J.*  
11 *Pharm. Biopharm.* **2016**, *98*, 57–66, DOI 10.1016/j.ejpb.2015.11.002.  
12  
13  
14 (20) Gross, J.; Sadowski, G. Perturbed-Chain SAFT: An Equation of State Based on a  
15 Perturbation Theory for Chain Molecules. *Ind. Eng. Chem. Res.* **2001**, *40* (4),  
16 1244–1260, DOI 10.1021/ie0003887.  
17  
18  
19 (21) Okuniewski, M.; Padaszyński, K.; Domańska, U. (Solid + Liquid) Equilibrium Phase  
20 Diagrams in Binary Mixtures Containing Terpenes: New Experimental Data and  
21 Analysis of Several Modelling Strategies with Modified UNIFAC (Dortmund) and  
22 PC-SAFT Equation of State. *Fluid Phase Equilib.* **2016**, *422*, 66–77, DOI  
23 10.1016/j.fluid.2015.12.048.  
24  
25  
26 (22) Domalski, E. S.; Hearing, E. D. Heat Capacities and Entropies of Organic  
27 Compounds in the Condensed Phase. Volume III. *J. Phys. Chem. Ref. Data* **1996**,  
28 *25* (1), 1–525, DOI 10.1063/1.555985.  
29  
30  
31 (23) Pontes, P. V. A.; Crespo, E. A.; Martins, M. A. R.; Silva, L. P.; Neves, C. M. S. S.;  
32 Maximo, G. J.; Hubinger, M. D.; Batista, E. A. C.; Pinho, S. P.; Coutinho, J. A. P.; et  
33 al. Measurement and PC-SAFT Modeling of Solid-Liquid Equilibrium of Deep  
34 Eutectic Solvents of Quaternary Ammonium Chlorides and Carboxylic Acids.  
35 *Fluid Phase Equilib.* **2017**, *448*, 69–80, DOI 10.1016/j.fluid.2017.04.007.  
36  
37  
38 (24) Misra, A. K.; Misra, M.; Panpalia, G. M.; Dorle, A. K. Thermoanalytical and  
39 Microscopic Investigation of Interaction between Paracetamol and Fatty Acid  
40 Crystals. *J. Macromol. Sci. Part A* **2007**, *44* (7), 685–690, DOI  
41 10.1080/10601320701351177.  
42  
43  
44 (25) Hong, J.; Hua, D.; Wang, X.; Wang, H.; Li, J. Solid-Liquid-Gas Equilibrium of the  
45 Ternaries Ibuprofen + Myristic Acid + CO<sub>2</sub> and Ibuprofen + Tripalmitin + CO<sub>2</sub>. *J.*  
46 *Chem. Eng. Data* **2010**, *55* (1), 297–302, DOI 10.1021/je900342a.  
47  
48  
49  
50  
51  
52  
53  
54  
55  
56  
57  
58  
59  
60

- 1  
2  
3 (26) Schneider, H.; Badrieh, Y.; Migron, Y.; Marcus, Y. Hydrogen Bond Donation  
4 Properties of Organic Solvents and Their Aqueous Mixtures from  $^{13}\text{C}$  NMR Data  
5 of Pyridine-*n*-Oxide. *Zeitschrift für Phys. Chemie* **1992**, *177* (2), 143–156, DOI  
6 10.1524/zpch.1992.177.Part\_2.143.  
7  
8  
9  
10 (27) Teles, A. R. R.; Capela, E. V.; Carmo, R. S.; Coutinho, J. A. P.; Silvestre, A. J. D.;  
11 Freire, M. G. Solvatochromic Parameters of Deep Eutectic Solvents Formed by  
12 Ammonium-Based Salts and Carboxylic Acids. *Fluid Phase Equilib.* **2017**, *448*, 15–  
13 21, DOI 10.1016/j.fluid.2017.04.020.  
14  
15  
16  
17 (28) Schröder, B.; Martins, M. A. R. R.; Coutinho, J. A. P. P.; Pinho, S. P. Aqueous  
18 Solubilities of Five N-(Diethylaminothiocarbonyl)Benzimido Derivatives at  
19  $T = 298.15\text{ K}$ . *Chemosphere* **2016**, *160*, 45–53, DOI  
20 10.1016/j.chemosphere.2016.06.042.  
21  
22  
23  
24 (29) Prausnitz, J. M.; Lichtenthaler, R. N.; Azevedo, E. G. *Molecular Thermodynamics*  
25 *Fluid Phase Equilibria*; Prentice-Hall, 1986.  
26  
27  
28 (30) Gmehling, J.; Kolbe, B.; Kleiber, M.; Rarey, J. *Chemical Thermodynamics for*  
29 *Process Simulation*; Wiley-VCH, 2012.  
30  
31  
32 (31) Coutinho, J. A. P.; Andersen, S. I.; Stenby, E. H. Evaluation of Activity Coefficient  
33 Models in Prediction of Alkane Solid-Liquid Equilibria. *Fluid Phase Equilib.* **1995**,  
34 *103* (1), 23–39, DOI 10.1016/0378-3812(94)02600-6.  
35  
36  
37  
38 (32) Hendriks, E. M. Applied Thermodynamics in Industry, a Pragmatic Approach.  
39 *Fluid Phase Equilib.* **2011**, *311*, 83–92, DOI 10.1016/J.FLUID.2010.07.019.  
40  
41  
42 (33) Passos, H.; Khan, I.; Mutelet, F.; Oliveira, M. B.; Carvalho, P. J.; Santos, L. M. N. B.  
43 F.; Held, C.; Sadowski, G.; Freire, M. G.; Coutinho, J. A. P. Vapor-Liquid Equilibria  
44 of Water plus Alkylimidazolium-Based Ionic Liquids: Measurements and  
45 Perturbed-Chain Statistical Associating Fluid Theory Modeling. *Ind. Eng. Chem.*  
46 *Res.* **2014**, *53* (9), 3737–3748, DOI 10.1021/ie4041093.  
47  
48  
49  
50 (34) Crespo, E. A.; Silva, L. P.; Martins, M. A. R.; Fernandez, L.; Ortega, J.; Ferreira, O.;  
51 Sadowski, G.; Held, C.; Pinho, S. P.; Coutinho, J. A. P. Characterization and  
52 Modeling of the Liquid Phase of Deep Eutectic Solvents Based on Fatty  
53 Acids/Alcohols and Choline Chloride. *Ind. Eng. Chem. Res.* **2017**, *56* (42), 12192–  
54  
55  
56  
57  
58  
59  
60

- 12202, DOI 10.1021/acs.iecr.7b02382.
- (35) Padiuszyński, K.; Okuniewski, M.; Domańska, U. "Sweet-in-Green" Systems Based on Sugars and Ionic Liquids: New Solubility Data and Thermodynamic Analysis. *Ind. Eng. Chem. Res.* **2013**, *52* (51), 18482–18491, DOI 10.1021/ie4033186.
- (36) Jackson, G.; Chapman, W. G.; Gubbins, K. E. Phase Equilibria of Associating Fluids of Spherical and Chain Molecules. *Int. J. Thermophys.* **1988**, *9* (5), 769–779, DOI 10.1007/BF00503243.
- (37) Chapman, W. G.; Jackson, G.; Gubbins, K. E. Phase Equilibria of Associating Fluids Chain Molecules with Multiple Bonding Sites. *Mol. Phys.* **1988**, *65* (5), 1057–1079, DOI 10.1207/s15327752jpa8502.
- (38) Chapman, W. G.; Gubbins, K. E.; Jackson, G.; Radosz, M. SAFT: Equation-of-State Solution Model for Associating Fluids. *Fluid Phase Equilib.* **1989**, *52*, 31–38, DOI 10.1016/0378-3812(89)80308-5.
- (39) Chapman, W. G.; Gubbins, K. E.; Jackson, G.; Radosz, M. New Reference Equation of State for Associating Liquids. *Ind. Eng. Chem. Res.* **1990**, *29* (8), 1709–1721, DOI 10.1021/ie00104a021.
- (40) Wertheim, M. S. Fluids with Highly Directional Attractive Forces. I. Statistical Thermodynamics. *J. Stat. Phys.* **1984**, *35* (1), 19–34, DOI 10.1007/BF01017362.
- (41) Wertheim, M. S. Fluids with Highly Directional Attractive Forces. II. Thermodynamic Perturbation Theory and Integral Equations. *J. Stat. Phys.* **1984**, *35* (1), 35–47, DOI 10.1007/BF01017363.
- (42) Wertheim, M. S. Fluids with Highly Directional Attractive Forces. III. Multiple Attraction Sites. *J. Stat. Phys.* **1986**, *42* (3), 459–476, DOI 10.1007/BF01127721.
- (43) Wertheim, M. S. Fluids with Highly Directional Attractive Forces. IV. Equilibrium Polymerization. *J. Stat. Phys.* **1986**, *42* (3), 477–492, DOI 10.1007/BF01127722.
- (44) Gross, J.; Sadowski, G. Application of the Perturbed-Chain SAFT Equation of State to Associating Systems. *Ind. Eng. Chem. Res.* **2002**, *41*, 5510–5515, DOI 10.1021/ie010954d.
- (45) Verevkin, S. P.; Sazonova, A. Y.; Frolkova, A. K.; Zaitsau, D. H.; Prikhodko, I. V.;

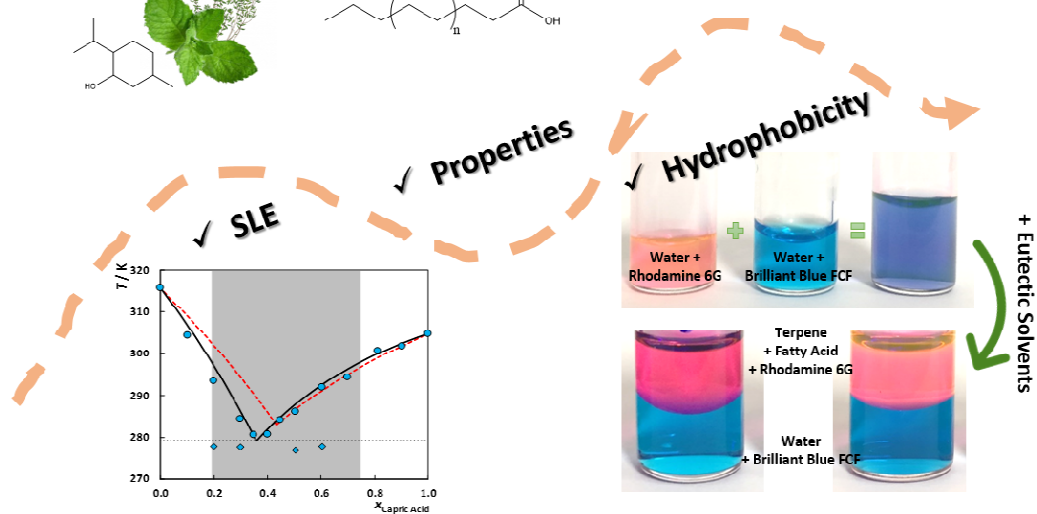
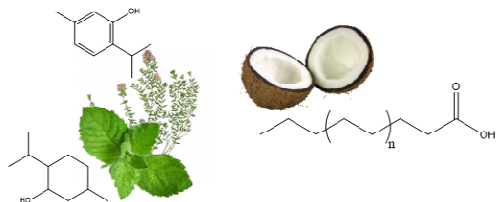
- 1  
2  
3 Held, C. Separation Performance of BioRenewable Deep Eutectic Solvents. *Ind.*  
4 *Eng. Chem. Res.* **2015**, *54* (13), 3498–3504, DOI 10.1021/acs.iecr.5b00357.  
5  
6  
7 (46) Zubeir, L. F.; Held, C.; Sadowski, G.; Kroon, M. C. PC-SAFT Modeling of CO<sub>2</sub>  
8 Solubilities in Deep Eutectic Solvents. *J. Phys. Chem. B* **2016**, *120* (9), 2300–2310,  
9 DOI 10.1021/acs.jpcc.5b07888.  
10  
11  
12 (47) Ashworth, C. R.; Matthews, R. P.; Welton, T.; Hunt, P. A. Doubly Ionic Hydrogen  
13 Bond Interactions within the Choline Chloride–urea Deep Eutectic Solvent. *Phys.*  
14 *Chem. Chem. Phys.* **2016**, *18* (27), 18145–18160, DOI 10.1039/C6CP02815B.  
15  
16  
17 (48) Martins, M. A. R.; Carvalho, P. J.; Palma, A. M.; Domańska, U.; Coutinho, J. A. P.;  
18 Pinho, S. P. Selecting Critical Properties of Terpenes and Terpenoids through  
19 Group-Contribution Methods and Equations of State. *Ind. Eng. Chem. Res.* **2017**,  
20 *56* (35), 9895–9905, DOI 10.1021/acs.iecr.7b02247.  
21  
22  
23 (49) Carvalho, P. J.; Regueira, T.; Santos, L. M. N. B. F.; Fernandez, J.; Coutinho, J. A.  
24 P. Effect of Water on the Viscosities and Densities of 1-Butyl-3-  
25 Methylimidazolium Dicyanamide and 1-Butyl-3-Methylimidazolium  
26 Tricyanomethane at Atmospheric Pressure. *J. Chem. Eng. Data* **2009**, *55* (2),  
27 645–652, DOI 10.1021/je900632q.  
28  
29  
30 (50) Wang, X.; Sun, T.; Teja, A. S. Density, Viscosity, and Thermal Conductivity of  
31 Eight Carboxylic Acids from (290.3 to 473.4) K. *J. Chem. Eng. Data* **2016**, *61* (8),  
32 2651–2658, DOI 10.1021/acs.jced.5b00971.  
33  
34  
35 (51) Cedeño González, F. O.; Prieto González, M. . M.; Bada Gancedo, J. C.; Alonso  
36 Suárez, R.; Suárez, R. A. Estudio de La Densidad y de La Viscosidad de Algunos  
37 Ácidos Grasos Puros. *Grasas y Aceites* **1999**, *50* (5), 359–368, DOI  
38 10.3989/gya.1999.v50.i5.680.  
39  
40  
41 (52) Martins, M. A. R.; Neves, C. M. S. S.; Kurnia, K. A.; Carvalho, P. J.; Rocha, M. A. A.;  
42 Santos, L. M. N. B. F.; Pinho, S. P.; Freire, M. G. Densities, Viscosities and Derived  
43 Thermophysical Properties of Water-Saturated Imidazolium-Based Ionic Liquids.  
44 *Fluid Phase Equilib.* **2015**, *407*, 188–196, DOI 10.1016/j.fluid.2015.05.023.  
45  
46  
47 (53) Okoturo, O. O.; VanderNoot, T. J. Temperature Dependence of Viscosity for  
48 Room Temperature Ionic Liquids. *J. Electroanal. Chem.* **2004**, *568*, 167–181, DOI  
49  
50  
51  
52  
53  
54  
55  
56  
57  
58  
59  
60

1  
2  
3 10.1016/j.jelechem.2003.12.050.  
4

- 5 (54) Florindo, C.; McIntosh, A. J. S.; Welton, T.; Branco, L. C.; Marrucho, I. M. A Closer  
6 Look into Deep Eutectic Solvents: Exploring Intermolecular Interactions Using  
7 Solvatochromic Probes. *Phys. Chem. Chem. Phys.* **2017**, *20* (1), 206–213, DOI  
8 10.1039/C7CP06471C.  
9  
10  
11  
12 (55) Yalkowsky, S. H.; He, Y.; Jain, P. *Handbook of Aqueous Solubility Data*, 2nd ed.;  
13 CRC Press, 2010.  
14  
15  
16  
17  
18  
19  
20  
21  
22  
23  
24  
25  
26  
27  
28  
29  
30  
31  
32  
33  
34  
35  
36  
37  
38  
39  
40  
41  
42  
43  
44  
45  
46  
47  
48  
49  
50  
51  
52  
53  
54  
55  
56  
57  
58  
59  
60

## TOC/Abstract Graphic

## Terpenes + Fatty Acids



## Synopsis

Characterization of sustainable hydrophobic eutectic solvents formed by terpenes and monocarboxylic acids.